Local stress gradient approach for multiaxial fatigue behaviour assessment of high strength steels in occurrence of defects

Fabienne Pennec, Wichian Niamchaona, Kevin Tihay, Michel Duchet, Bastien Weber, Jean-Louis Robert

Available online at www.sciencedirect.com

ScienceDirect

Procedia Engineering 213 (2018) 662–673

Procedia Engineering

www.elsevier.com/locate/procedia

7th International Conference on Fatigue Design, Fatigue Design 2017, 29-30 November 2017, Senlis, France

Local stress gradient approach for multiaxial fatigue behaviour assessment of high strength steels in occurrence of defects

Fabienne Pennec[a,*], Wichian Niamchaona[a], Kevin Tihay[b], Michel Duchet[b], Bastien Weber[b], Jean-Louis Robert[a]

[a]*Université Clermont Auvergne, Institut Pascal, BP 10448, F-63000 Clermont-Ferrand, France*
[b]*ArcelorMittal Maizières Research SA BP 30320 Voie Romaine 57283 Maizières-Les-Metz Cedex, France*

Abstract

This study is dedicated to the effect of surface defects on the fatigue behaviour of high strength steels and the evaluation of their sensitivity. For that purpose, defects were introduced by Electro-Discharge Machining (EDM) on the edge of sheet metal test samples. Different defect depths are tested on high strength steel grades. A stress-based multiaxial fatigue life prediction method is then developed to assess the fatigue life. Input data are cyclic stress tensor states at the notch root that are calculated by a FEM analysis using the open-source Salome-meca software. In fact elastic–plastic numerical simulations were performed for each defect geometry to determine stresses distribution around the defect. A new class of multiaxial fatigue criteria extended from classical formulation to new ones with stress gradient terms related to the normal stress component is formulated. The Fogue integral approach based criterion is used since it is proved to give pertinent prevision under rotating principal stress directions multiaxial loading. For any material plane P the local stress gradient in its normal direction is calculated by parabolic interpolation and integrated to the normal stress component within the multiaxial fatigue criterion. For investigated multiaxial criteria, accounting for stress gradient effect is assessed from the experimental campaign results on two very high strength steel grades with occurence of surface defects.

Peer-review under responsibility of the scientific committee of the 7th International Conference on Fatigue Design.

Keywords: high strength steel; defect ; multiaxial fatigue criterion; stress gradient

* Corresponding author. Tel.: +33 4 70 02 20 98.
E-mail address: fabienne.pennec@uca.fr

1877-7058
Peer-review under responsibility of the scientific committee of the 7th International Conference on Fatigue Design.
10.1016/j.proeng.2018.02.062

1. Introduction

Because of economic constraints, there is a strong requirement nowadays for making decrease the material weight of mechanical structures; hence the stress levels induced by the service loading are increasing. The introduction of Very High Strength Steels provides by this way lightweight design and allows cost saving. The VHSS fatigue strength increases with mechanical properties but steel grades becomes also more sensitive to defects. Many industrial components such as chassis parts contain namely defects of different kinds (scratch, sharp notch or sensitivity viewed as defects such as coating thickness, cut edge…). As these surface defects of high strength steels have been shown to be the origin of the failure under cyclic loading, understanding the fatigue process and assessing its effects for engineering components or structures are of great importance for mechanical design in order to guarantee an appropriate in-service durability. Different approaches have been proposed in the literature for materials containing defects. They can be classified into three main groups: empirical approach, approach based on fatigue notch factor and fracture mechanics approach.

Murakami and Endo [1] developed an interesting empirical approach and defined the so-called parameter $\sqrt{area}$ as defect size parameter which is the square root of the surface of the defect in the plane perpendicular to the maximum principal stress direction [2]. Murakami and Endo finally proposed an equation for fatigue limit including location of the defects (surface, internal), stress ratio R and the material hardness H_v whereas no consideration is made about the defect shape. This approach has been largely validated for different metallic materials under uniaxial conditions. Problems emerge for complex loading or cyclic plasticity. Even if the defect size includes the loading direction, the use of the maximum principal stress is not sufficient because of the lack of consideration of the stress triaxiality [3].

Other authors [4, 5] proposed to calculate the fatigue limit by assuming that the defect is a notch. Stress concentration factors K_t are often used to describe the effect of notches [6, 7]. They estimate the stress amplification in the vicinity of the geometric discontinuity in the case of linear elastic areas [4, 5]. Under cyclic loading, fatigue concentration factors K_f were introduced first in the 1950s and related to stress concentration factors K_t by means of empirical relations [8, 9]. These approaches are useful only for materials and loading conditions for which the multiaxiality effect of loading is not observed. Moreover the stress gradient is not directly taken into account.

The fracture mechanics approach considers the defects as pre-existent cracks. The fatigue limit is calculated using the strength intensity factor concept, by using the relevant crack threshold ΔK_{th}, the crack shape factor Y and the crack length. These parameters may be difficult to determine especially in the case of complex defect shape and multiaxial loading. This approach gives good results for conservative design under uniaxial tension loading and becomes inadequate in the case of multiaxial loading [10, 3]. Besides, this concept assumes on the one hand that the initiation stage is negligible and on the other hand that the propagation from the defect to final failure controls the fatigue life.

Nomenclature

a, b, d	material parameters of Fogue's criterion
δ	material parameter of modified Fogue's criterion
ΔK_{th}	crack threshold
E_{FOGUE}	Fogue's fatigue function
E_h	material plane damage indicator
G	normal stress gradient
[G]	stress gradient tensor
h	unit normal vector to a material plane
H_v	Vickers hardness
N	lifetime (number of cycles)
R	stress ratio ($R = \sigma_{min}/\sigma_{max}$)
R_m	ultimate tensile strength
$R_{p0.2}$	monotonic yield stress
S	sphere area which radius is equal to unit (S=4π)

σ_{-1}	fatigue limit under fully reversed tensile test (R=-1)
σ_0	fatigue limit under zero to maximum tensile test (R=0)
$\sigma_{0.1}$	fatigue limit under tension – tension test with R=0.1
σ_{hha}	normal stress amplitude on the h-normal material plane
σ_{hhm}	mean value of the normal stress
σ_{hh}	normal stress
τ_{ha}	shear stress amplitude acting on the h-normal material plane
τ_{-1}	Fatigue limit under fully reversed torsion test (R=-1)

Fig. 1 illustrates an example of Kitagawa diagram obtained for Dual Phase steel specimens with defect of various sizes similar to crack of various depths and introduced on the specimen flange. Tensile fatigue tests (R=0.1) have been conducted by ArcelorMittal. The diagram highlights the defect size influence on the fatigue limit and shows that a high strength steel is highly sensitive to machined defect size. Three linear characteristics are added to the graph: the fatigue limit of smooth material, the Murakami threshold and two crack thresholds determined by ArcelorMittal from experimental tests ($3.5\ \text{MPa}\sqrt{m} \leq \Delta K_{th} \leq 5\ \text{MPa}\sqrt{m}$). Cracks thresholds give conservative results while Murakami approach does not agree with experimental results.

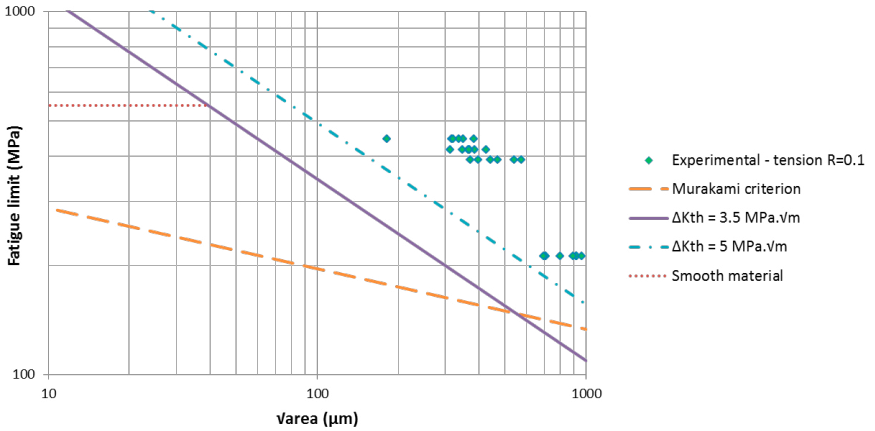

Fig. 1. Kitagawa diagram for a DP steel grade under tension-tension fatigue test.

Another non-local approach exists and is based on the stress gradient generated by the defect [11, 12]. Stresses fields obtained from the Finite Elements Method allow considering any type, shape and size of defect. This approach is available under multiaxial conditions by using a multiaxial fatigue criterion with stress gradient consideration. Papadopoulos [13] used this method by adding a stress gradient term in Matake criterion [14]. The gradient of the normal stress is calculated for its maximal value on the criterion critical plane. Billaudeau [11] modified the Crossland criterion [15] to describe the fatigue behaviour of defective metallic materials by introducing the gradient of the hydrostatic stress. Predictions obtained with modified Crossland criterion have however a non-conservative trend while critical plane definition is contrary to the fatigue function expression in Papadopoulos approach [16].

The objective of this paper is to propose a relevant mechanical approach in the general case of various defect geometries and multiaxial loading. In this way the stress distribution around defect is determined performing elastic-plastic simulations and a gradient based multiaxial fatigue failure criterion is used to estimate the fatigue limit. Instead of the Crossland criterion or the Matake criterion a fatigue criterion based on the so called global approach is used. On the contrary to Billaudeau's proposal, the stress gradient effect of the proposed method is considered not in a single direction but on any material plane. The normal stress gradient is taken into account for that purpose.

2. Experimental results

The tested material is a Complex Phase steel CP800 (Table 1) that is cold formed to make lightweight structural elements. This steel offers high as-delivered yield strength and good bendability and stretch flangeability. It is particularly well suited for automotive safety components requiring good impact strength and for suspension system components. Fatigue tests are performed on shouldered test bars (2 mm thickness specimens). The minimal width of the specimens tested in this study is 18 mm. This geometry generates a low stress concentration factor (1.06). Tensile fatigue tests were conducted by ArcelorMittal at 30 Hz using a fatigue testing machine. Tests were firstly conducted on the defect free material (i.e. smooth specimens) in order to determine the reference fatigue limit at $2x10^6$ cycles.

Table 1. Mechanical properties of CP800 steel.

Young's modulus (MPa)	200000
Ultimate tensile strength: Rm (MPa)	881.47
Monotonic yield stress: $R_{p0.2}$ (MPa)	819.96
Elongation rate: A (%)	18.33
Fatigue limit ($2x10^6$ cycles ; R=0.1) (MPa)	675
Fatigue limit ($2x10^6$ cycles ; R=-1) (MPa)	362

Artificial defects with controlled size (from 10 µm to 300 µm) have been introduced on the flange of fatigue samples by electrical discharge machining (EDM) using a 200 µm diameter wire (Fig. 2 and 3). Each size is not common for the four defect types as the smallest ones were difficult to machine in a reproducible manner. The Table 2 summarizes the mean value and standard deviation of kept defect depths for the experimental fatigue tests.

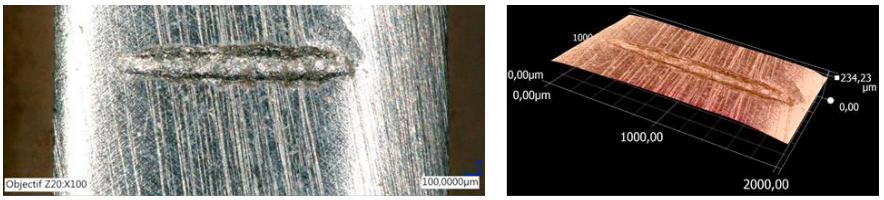

(a) (b)

Fig. 2. (a) Observation of the defect introduced by EDM on the flange of the VHS steel (DP780HR); (b) 3D reconstruction.

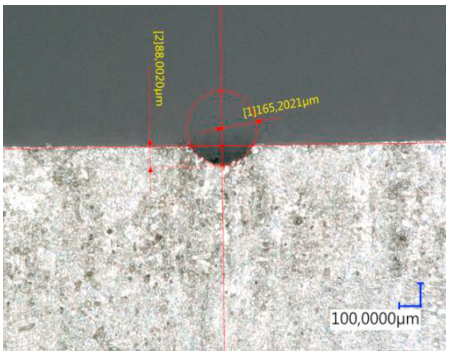

Fig. 3. Measurement of the defect geometry introduced by EDM on the flange of CP800 grade specimen.

Fatigue tests were conducted under tension-tension loading with a load ratio R equal to 0.1 on ten specimens in order to estimate the fatigue strength at $2x10^6$ cycles. Fig. 4 represents the obtained experimental data and the respective Basquin model equations [17].

Table 2. Four defect types characterization.

Depth (µm)	Mean value (µm)	Standard deviation (µm)
31	31.4	5.1
67	66.6	7.2
127	126.7	6.8
297	297.3	14.8

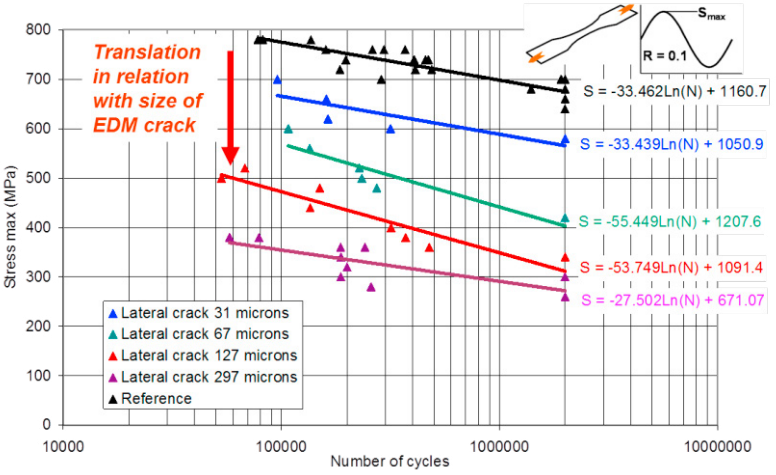

Fig. 4. Reference and defect affected SN curves for a CP800 steel under tensile cyclic loads.

3. Calculated local stresses at the defect tip

Finite element method was used to compute the stress states distribution around the defects. The models have been generated in the Salome-Meca 2016 environment by using the scripting python. Simulations have been conducted for each size of defect. Symmetry and boundary conditions are directly representative of the fatigue sample. Ten loadings were applied in accordance with the experimental cyclic loading ratio (R=0.1) and allowed building the minimum circumscribed circle to determine the key stress parameters in the proposed mechanical approach.

Tetrahedral solid elements with higher mesh density in the vicinity of defect were used for the computations. In order to obtain an appropriate mesh structure that may enable accurate calculation of the stress states, a convergence analysis was carried out for the element size. For all the defects, the critical point is located at the crack tip. A particular attention is hence paid for meshing close to the defect tip at the calculation point M where the stress gradient is assessed. A mesh size of about 3 µm is hence selected in the notch vicinity (Fig. 5).

As the maximum value of the Von Mises stress in elastic simulations exceeds the yield stress for almost any model, elastic–plastic simulations were performed in Code_Aster by using the engineering stress-strain response of CP800 steel (Fig. 6). In default of the cyclic hardening model of the material, an isotropic hardening law with a yield surface defined by the Von Mises criterion (VMIS_ISOT_TRAC) has been selected, which allows a comparative analysis between the different defects.

Fig. 7 shows the distribution of the six stress components (σ_{xx}, σ_{yy}, σ_{zz}, σ_{xy}, σ_{xz}, σ_{yz}) as a function of the distance from the 127 µm depth notch root along x and y axes. The stress state has been determined via the elasto-plastic FE analysis with a load value corresponding to the fatigue limit at $2x10^6$ cycles. The distribution of these components for the other sizes and the other geometries show the same trends, whereby the normal tensile stress σ_{yy} is always the greatest at notch root. Significant evolution from point M to the bulk material is observed. The stress gradient is also

not constant along the plotted lines. A rigourous method presented in the subsection 4.3 is used to assess the stress gradient of each component at the critical point M where crack initiates under fatigue tensile loading.

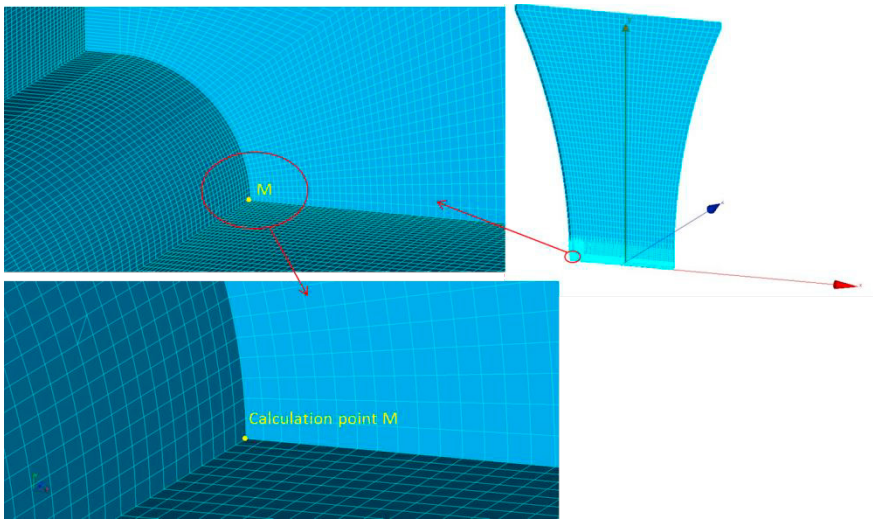

Fig.5. Meshing of the fatigue sample and detail of the mesh at the tip of the 127 µm depth defect.

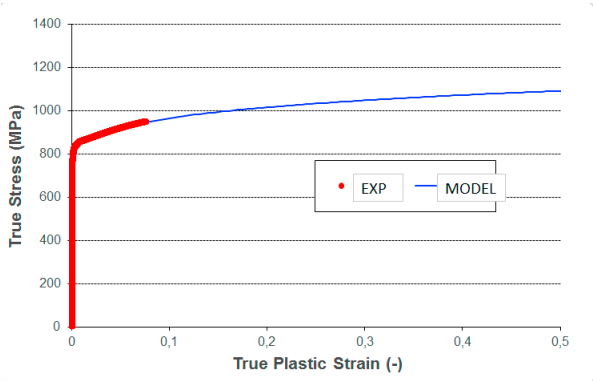

Fig.6. CP800 stress-strain response curve.

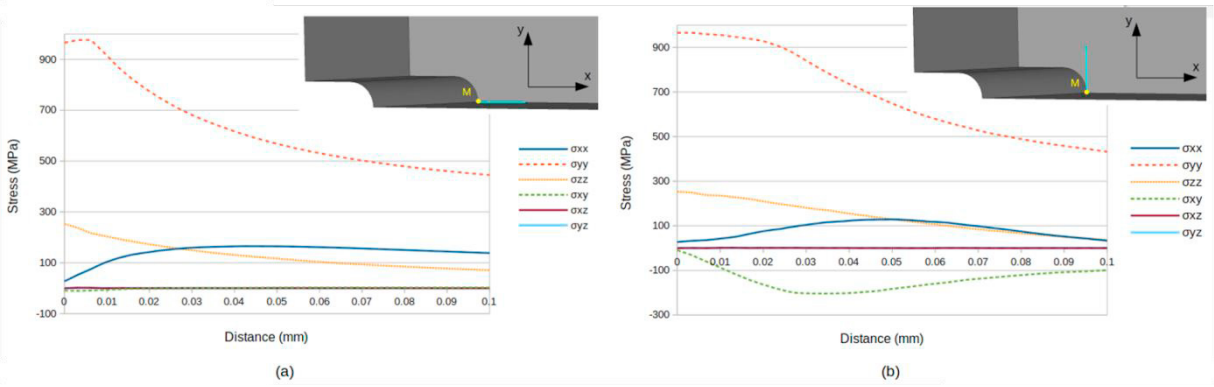

Fig.7. Distribution of the six stress components determined for the applied load corresponding to the fatigue limit at $2x10^6$ cycles as a function of the distance from the notch root for a size of 127 µm, (a) along x-axis; (b) along y-axis.

4. Multiaxial fatigue criterion

4.1. Basic fatigue criterion

Since the stress state at the notch root is not uniaxial, a suitable multiaxial fatigue approach has to be used. This criterion is applied at the surface of the defect where a crack is most likely to occur.

The multiaxial fatigue criterion proposed by Fogue [18] in 1987 is used as a basis. According to this author the damage indicator related to one material plane has to be considered as a linear combination of mean values and amplitudes of shear and normal stress components acting on this plane during the cycle:

$$E_h = \frac{a\,\tau_{ha} + b\,\sigma_{hha} + d\sigma_{hhm}}{\sigma_{-1}} \tag{1}$$

where a, b and d are criterion parameters depending on material fatigue limits σ_{-1}, τ_{-1} and σ_0. They are determined by stating that the criterion is checked (E_{Fogue}=1) for these three basic fatigue strengths cycles. The author states then the quadratic mean value all over the possible material planes for assessing the fatigue function E_{Fogue} of the material with respect to the multiaxial analysed cycle.

$$E_{Fogue} = \sqrt{\frac{1}{S}\int_S {E_h}^2 dS} \tag{2}$$

where S is the area of a unit radius sphere.

A previous work [19] has shown that one criterion based on the critical plane approach is especially suitable when principal stress directions remain fixed during the cycle, as the most activated slipped plane is always the same. The global approach gives the best description of the material fatigue behavior when principal stress directions rotate during the cycle, because in that case several slipping plane are generally activated. The root mean square, which makes a quadratic average of the fatigue damage indicator per plane E_h, is a way to take into account that physical phenomenon. Fig. 8 gives an example for the distribution of the calculated fatigue indicator deviations (E-1) by Weber [20] for the Fogue criterion and Dang Van criterion, for fixed principal stress directions cycles and rotating principal stress directions cycles respectively.

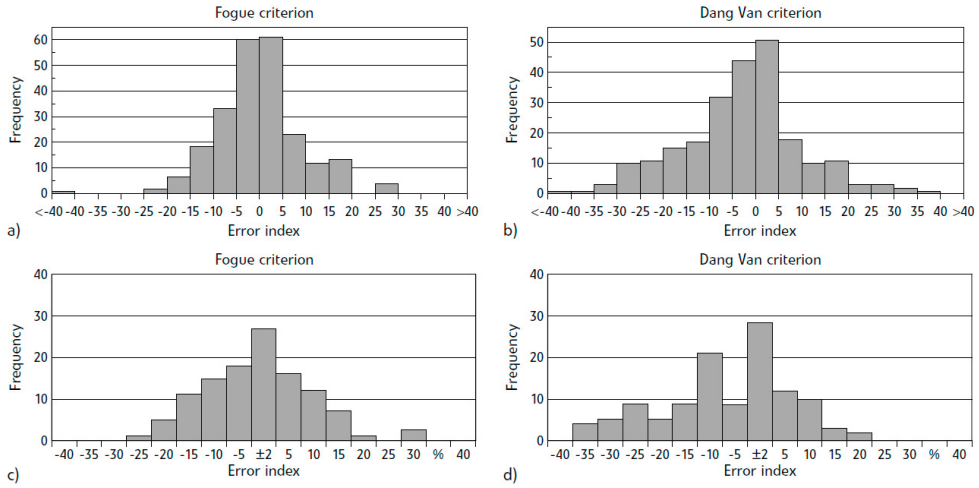

Fig. 8. Distribution of the calculated damage indicator deviations (E -1) for the Fogue and Dang Van Criterion; (a, b) Fixed principal stress directions; (c, d) Rotating principal stress directions [20].

Recall that in this paper the criterion parameters are identified by using two reference fatigue limits for smooth specimens, at $2x10^6$ cycles, one is determined under purely reversed tensile loads (R=-1) and the other one under tensile-tensile load (R=0.1). Note that the repeated tensile fatigue limit has been estimated using the Haigh diagram modeled by Gerber's parabola. The fatigue limit τ_{-1} under purely reversed torsion is deduced from the purely reversed tensile fatigue limit σ_{-1} by using Eq.3:

$$\tau_{-1} = \frac{\sigma_{-1}}{\sqrt{3}} \tag{3}$$

4.2. Approach accounting for stress gradient

The effect of the macroscopic stress gradient is obvious well known in fatigue and is known to be beneficial to the fatigue strength, whereas the stress concentration induced by geometry proves to be detrimental.

Papadopoulos [13] proposed a criterion including stress gradient effect after an experimental analysis. He concludes that the gradient effect is one order of magnitude higher than pure size effect. Luu [21] proposed new class of criteria to capture both well-known phenomena "Smaller is Stronger" and "Higher gradient is Stronger". According to Luu and basing on some experimental observations "Smaller is Stronger" is related to pure size and above all to gradient effect.

While Papadopoulos [13] and Billaudeau [11] concludes that the gradient of the deviatoric part of the stress distribution is not influent, Luu [21] and Zepeng [22] proposed to take into account both gradients related to normal stress part and shear stress part. They justify their approach based on bending-torsion fatigue tests and show some deviation between the modified multiaxial fatigue criteria proposed by Papadopoulos and the new class of fatigue criteria with both gradient terms in the "Papadopoulos ellipse arc" equation. However the plotted Papadopoulos curve with gradient does not seem to correspond to the curve obtained by Papadopoulos in [13], whereas the material data are the same and are related to the SAE 4340 steel [23]. A deviation of 20 MPa is notably observed on τ_{-1}.

In this paper the hypothesis is made that the stress gradient of the shear part of the stress tensor does not influence the fatigue limit. The proposed criterion only includes hence the gradient of the normal stress.

4.3. Stress gradient assessment method

The stress distribution for all defects is analyzed with a particular attention to the role of the normal stress spatial evolutions. Materials with defect are treated with the same basic mechanisms than defect-free materials. The purpose is consequenly to calculate the gradient of the normal stress σ_{hh} at the calculation point M by using the definition of the geometrical gradient given by Papadopoulos [13]:

$$G_1 = \sqrt{\left(\frac{\partial \sigma_{hhmax}}{\partial x}\right)^2 + \left(\frac{\partial \sigma_{hhmax}}{\partial y}\right)^2 + \left(\frac{\partial \sigma_{hhmax}}{\partial z}\right)^2} \tag{4}$$

We propose to give another definition of the gradient in the vicinity of the defect at point M:

$$G_2 = \sqrt{\left(\frac{\partial \sigma_{hhmax}}{\partial h}\right)^2} \tag{5}$$

As seen in Fig. 7, the stress gradient is not constant along the plotted lines. It is necessary to find the definition of the stress gradient calculation. The purpose is to use the following relations:

$$\frac{\partial \sigma_{hhmax}}{\partial h} = h_x \frac{\partial \sigma_{hhmax}}{\partial x} + h_y \frac{\partial \sigma_{hhmax}}{\partial y} + h_z \frac{\partial \sigma_{hhmax}}{\partial z} \tag{6}$$

with:

$$\frac{\partial \sigma_{hh}}{\partial x} = h_x^2 \frac{\partial \sigma_{xx}}{\partial x} + h_y^2 \frac{\partial \sigma_{yy}}{\partial x} + h_z^2 \frac{\partial \sigma_{zz}}{\partial x} + 2h_x h_y \frac{\partial \sigma_{xy}}{\partial x} + 2h_x h_z \frac{\partial \sigma_{xz}}{\partial x} + 2h_y h_z \frac{\partial \sigma_{yz}}{\partial x} \quad (7)$$

$$\frac{\partial \sigma_{hh}}{\partial y} = h_x^2 \frac{\partial \sigma_{xx}}{\partial y} + h_y^2 \frac{\partial \sigma_{yy}}{\partial y} + h_z^2 \frac{\partial \sigma_{zz}}{\partial y} + 2h_x h_y \frac{\partial \sigma_{xy}}{\partial y} + 2h_x h_z \frac{\partial \sigma_{xz}}{\partial y} + 2h_y h_z \frac{\partial \sigma_{yz}}{\partial y} \quad (8)$$

$$\frac{\partial \sigma_{hh}}{\partial z} = h_x^2 \frac{\partial \sigma_{xx}}{\partial z} + h_y^2 \frac{\partial \sigma_{yy}}{\partial z} + h_z^2 \frac{\partial \sigma_{zz}}{\partial z} + 2h_x h_y \frac{\partial \sigma_{xy}}{\partial z} + 2h_x h_z \frac{\partial \sigma_{xz}}{\partial z} + 2h_y h_z \frac{\partial \sigma_{yz}}{\partial z} \quad (9)$$

$$[G] = \begin{bmatrix} \frac{\partial \sigma_{xx}}{\partial x} & \frac{\partial \sigma_{yy}}{\partial x} & \frac{\partial \sigma_{zz}}{\partial x} & \frac{\partial \sigma_{xy}}{\partial x} & \frac{\partial \sigma_{xz}}{\partial x} & \frac{\partial \sigma_{yz}}{\partial x} \\ \frac{\partial \sigma_{xx}}{\partial y} & \frac{\partial \sigma_{yy}}{\partial z} & \frac{\partial \sigma_{zz}}{\partial y} & \frac{\partial \sigma_{xy}}{\partial y} & \frac{\partial \sigma_{xz}}{\partial y} & \frac{\partial \sigma_{yz}}{\partial y} \\ \frac{\partial \sigma_{xx}}{\partial z} & \frac{\partial \sigma_{yy}}{\partial z} & \frac{\partial \sigma_{zz}}{\partial z} & \frac{\partial \sigma_{xy}}{\partial z} & \frac{\partial \sigma_{xz}}{\partial z} & \frac{\partial \sigma_{yz}}{\partial z} \end{bmatrix} \quad (10)$$

The gradient calculation in one given direction requires by this way the computation of the 18 components of the stress gradient tensor $[G]$ as written in Eq. 10. The numerical problem that has to be solved consists in determining, at the calculation point M, and for the applied load that corresponds to the experimental fatigue limit, the 18 partial derivatives. It is obvious that the numerical values accuracy will be strongly dependent on the finite elements size used to model the fatigue specimen in the defect vicinity.

The partial derivatives for one direction of the orthonormal basis are calculated using polynomial interpolation. As the crack initiation from the defect is a localized mechanism, second degree interpolation is made on the three first nodes of the meshing at the notch root. This method allows approximating the six stress components distributions from the defect tip (point M) along one direction of the 3D space and calculating at the calculation point M the six respective partial derivatives. Fig.9 illustrates the used method to determine the partial derivative of σ_{yy} along x-axis at point M for the fatigue specimen with a defect size of 127 µm. Once the 18 partial derivatives are calculated, Eq. 4 to 9 allow to assess the stress gradients G_1 and G_2 at the study point.

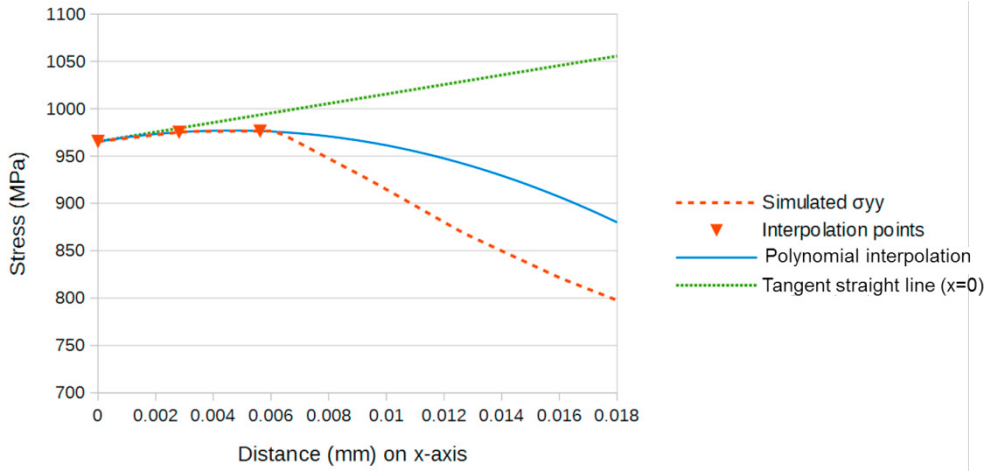

Fig. 9. Second degree polynomial interpolation method to determine the partial derivative $\partial\sigma_{yy}/\partial x$ at point M for a 127 µm defect size.

4.4. Multiaxial gradient criterion in occurrence of defects

The first multiaxial gradient criterion is derived from the Papadopoulos' work and has been proposed by Weber [16] for free defect materials.

$$E_{h1} = \frac{a\tau_{ha} + b\sigma_{hha} + d\sigma_{hhm} + \delta\sqrt{G_1}}{\sigma_{-1}(N)} \quad (11)$$

The second multiaxial gradient criterion is based on the formulation of gradient G_2.

$$E_{h2} = \frac{a\tau_{ha}+b\sigma_{hha}+d\sigma_{hhm}+\delta\sqrt{G_2}}{\sigma_{-1}(N)} \quad (12)$$

For both gradient fatigue criteria, the coefficient δ has to be identified by using one of the experimental results obtained for a fatigue specimen with an artificial defect. The CP800 specimen with the deepest lateral crack (297 µm) is selected in this study.

5. Analysis of the proposed multiaxial fatigue criteria

5.1. Results obtained from CP800 grade data

The new class of criteria based on the incorporation of the normal stress gradient to take into account the defect influence is tested at 2 million cycles using the CP800 experimental data. A comparison is made between the Fogue fatigue function calculated for each defect size without gradient and with gradient G_1 and G_2. Fig. 10 shows the Fogue fatigue function as a function of the defect size for the four defect geometries. For any defect the classical fatigue function is higher than the unit value, which shows that the calculated fatigue strengths are strongly bigger than the expected fatigue limits. The fatigue criteria based on the stress at the most loaded point, generally underestimate the fatigue life. On the contrary the gradient effect account significantly shifts all the experiment points toward the horizontal line (E_{FOGUE}=1), especially for the first formulation of the gradient G_1.

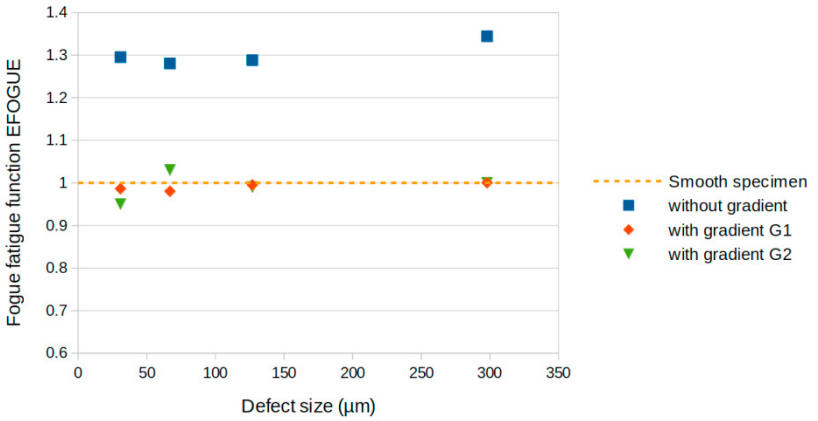

Fig. 10. Evolution of the fatigue function E_{FOGUE} at point M without gradient consideration and including gradient effect as a function of the defect size for CP800 steel material.

5.2. Validation on another very high strength steel

To confirm these first numerical results, a second study is conducted on a hot rolled ferrite-bainite steel FB540 (Table 3). Four types of artificial defects (37, 71, 130, 300 µm) have been introduced on the edge of 2.5 mm thickness specimens

Table 3. Mechanical properties of FB540 steel.

Ultimate tensile strength: Rm (MPa)	881.47
Monotonic yield stress: $R_{p0.2}$ (MPa)	458
Fatigue limit $\sigma_{0.1}$ ($2x10^6$ cycles) (MPa)	404
Fatigue limit σ_{-1} ($2x10^6$ cycles) (MPa)	246

Finite elements simulations were conducted using the FB540 cyclic elastic-plastic material behaviour. The experimental data have been obtained from Zhao's work [24].

Fatigue tests have been performed under tension loading with a loading ratio R equal to 0.1 on about ten specimens in order to estimate the fatigue strength at 2 million cycles. Fig. 11 represents the obtained experimental data and the respective Basquin model equations.

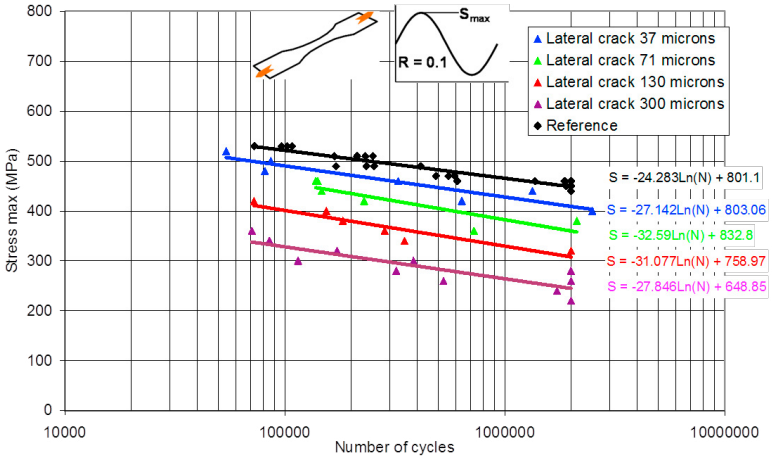

Fig. 11. Reference and defect affected SN curves for a FB540 steel under tensile-tensile load (R=0.1).

A comparison is then made between the Fogue fatigue function calculated for each defect size without gradient and with gradient G_1 and G_2 on Fig. 12. It shows that the classical Fogue fatigue criterion is not able to properly assess fatigue life of FB540 steel specimens when there is occurrence of defects. The introduction of the gradient effect correction significantly improves the fatigue life prediction of FB540 specimens with articial defects under tensile loads. An even slightly superior prediction is observed for the FB540 material compared to the CP800 material and may be attributed to the use of the cyclic elasto-plastic material behaviour law for FB540 steel grade.

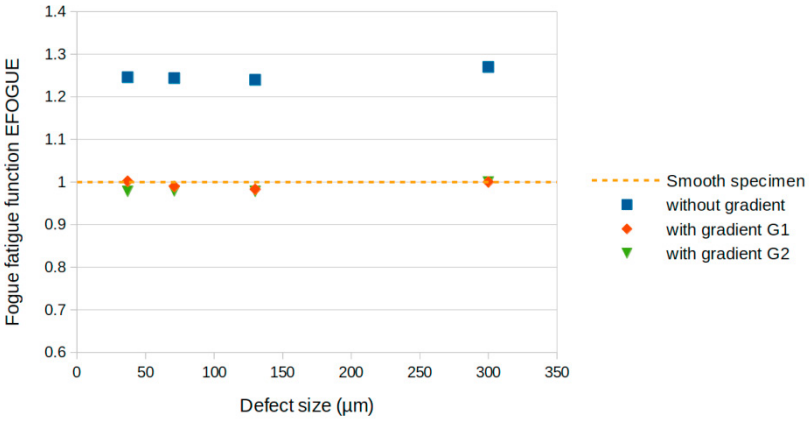

Fig. 12. Evolution of the fatigue function E_{FOGUE} at point M without gradient consideration and including gradients as a function of the defect size for FB540 steel material.

6. Conclusions

The non-gradient based approaches cannot perfectly assess fatigue life of very high strength steel specimens containing artificial defects on the flange. The stress concentration values in the crack vicinity are not able to correctly assess the local material fatigue strength. It is hence required to account for stress gradient considerations.

The approach proposed in this work shows the capacity to improve the endurance criterion predictions for tensile loading for any size of defects and for two steel grades. This may be due to many facts. Firstly an elastic-plastic material behaviour law has been used for stress states simulations. Secondly an integral approach criterion available for any multiaxial loading and that takes into account the damage of all material planes has been selected as a basis. Thirdly, a gradient effect correction has been introduced in the normal stress part. Finally the stress gradient is calculated at the defect tip by using its mathematical definition in any direction.

The developed approach allows also investigating the grade sensitivity to defects and provides an efficient tool that will further validated and improved. Only cases with critical points located at the crack tip have been examined, where the gradient is such that it has a beneficial effect on fatigue strength. The method has to be extended to all nodes of the finite element model. Moreover the proposed approach should be still applicable for any shapes of defect and any type of loading. The experimental campaign will be supplemented for such a purpose.

References

[1] Y. Murakami, M. Endo, Effects of defects, inclusions and inhomogeneities on fatigue strength, Int. J. Fatigue 16 (1994) 163–182.
[2] Y. Murakami, Metal fatigue : effects of small defects and nonmetallic inclusions. Elsevier; 2002.
[3]Y. Nadot, T. Billaudeau, Multiaxial fatigue limit criterion for defective materials, Eng. Fract. Mech. 73 (2006) 112–133.
[4] M.R. Mitchell, Review of the mechanical properties of cast steels with emphasis on fatigue behavior and the influence of microdiscontinuities, J. Eng. Mater. Technol., Trans. ASME (1977) 329–343.
[5] O. Lukas, L. Kunz, B. Weiss, R. Stickler, Non-damaging notches in fatigue, Fatigue Fract. Eng. Mater. Struct. 9 (1986) 195–204.
[6] R.E. Peterson, Design factors for stress concentrations, parts 1 to 5. Mach Des 1951(February–July).
[7] H. Neuber, Theoretical calculation of strength at stress concentration. Czechoslovak J Phys. 19 (3) (1969):400.
[8] E. Siebel, M. Stieler, Dissimilar stress distributions and cyclic loading. Z VerDeutsch Ing 97 (1955) 121–52.
[9] J.E. Shigley, C.R. Mischke, Mech Eng Des. New York: McGraw-Hill, Inc. (1989).
[10] Y. Nadot, J. Mendez, N. Ranganathan, Influence of casting defects on the fatigue limit of nodular cast iron, Int. J. Fatigue 26 (2004) 311–319.
[11] T. Billaudeau, Y. Nadot, G. Bezine, Multiaxial fatigue limit for defective materials: mechanisms and experiments, Acta Mater. 52 (2004) 3911–3920.
[12] A. Karolczuk, Y. Nadot, A. Dragon, Non-local stress gradient approach for multiaxial fatigue of defective material, Comput. Mat. Science 44 (2) (2008) 464-475.
[13] I.V. Papadopoulos, V.P. Panoskaltsis, Invariant formulation of a gradient dependent multiaxial high-cycle fatigue criterion, Eng. Fract. Mech. 55 (4) (1996) 513–528.
[14] T. Matake, An explanation on fatigue limit under combined stress, Bull. JSME 20 (141) (1977) 257–263.
[15] B. Crossland, Effect of large hydrostatic pressures on the torsional fatigue strength of an alloy steel - I.C.F.M. - IME/ASME (1956) 138-149.
[16] B. Weber, Fatigue multiaxiale des structures industrielles sous chargement quelconque, Thesis of the National Institute of Applied Sciences (INSA) of Lyon, Order number 99ISAL0056 (1999).
[17] O.H. Basquin, The exponential law of endurance tests, Proc ASTM, 10 (1910), 625-630.
[18] M. Fogue, Critère de fatigue à longue durée de vie pour des états multiaxiaux de contraintes sinusoïdales en phase et hors phase, Thesis of the National Institute of Applied Sciences (INSA) of Lyon, Order number 87ISAL0030 (1987).
[19] J.L. Robert, M. Fogue, J. Bahuaud, Fatigue life prediction under periodical or random multiaxial stress states, Automation in fatigue and fracture: testing and analysis, ASTM STP 1231 (edied by Amzallag C.), American Society for Testing and Materials, Philadelphia, (1994), 369-387.
[20] B. Weber, K. Ngargueudedjim, B. Soh Fotsing and J.L. Robert, On the efficiency of integral approach in multiaxial fatigue, Material prüfung 28 N°4 (2006) 156-159.
[21] D.H. Luu, H. Maitournam, Q.S. Nguyen, Formulation of gradient multiaxial fatigue criteria, Int. J. of Fatigue 61 (2014) 170-183
[22] M. Zepeng, P. Le Tallec, H. Maitournam, Multiaxial fatigue criteria with length scale and gradient effects, Procedia Engineering 133 (2015) 60-71.
[23] W.N. Findley, J.J. Coleman, B.C. Hanley, Theory for combined bending and torsion fatigue with data for SAE 4340 steel, Proc. Int. Conf. on Fatigue of Metals, I. Mech. E, London, England (1956) 150-157.
[24] Y. Zhao, M. Ma, R. Qin, Y. Ling, G. Wang, H. Gu, Y. Liu, A fabrication history based strain-fatigue model for prediction of crack initiation in a radial loading wheel, Fatigue Fract Engng Mater Struct (2017) 00 1–11